An optimized process design for oxymethylene ether production from woody-biomass-derived syngas

Xiaolei Zhang[1,3], Adetoyese Olajire Oyedun[1], Amit Kumar[1,1], Dorian Oestreich[2], Ulrich Arnold[2], Jörg Sauer[2]

[1]*Department of Mechanical Engineering, 10-263 Donadeo Innovation Centre for Engineering, University of Alberta, Edmonton, Alberta T6G 1H9,*

[2]*Institute of Catalysis Research and Technology (IKFT), Karlsruhe Institute of Technology (KIT), Hermann-von-Helmholtz-Platz 1, 76344 Eggenstein-Leopoldshafen, Germany.*

[3] *School of Mechanical and Aerospace Engineering, Queen's University Belfast, Belfast, BT9 5AH, UK.*

Abstract

The conversion of biomass for the production of liquid fuels can help reduce the greenhouse gas (GHG) emissions that are predominantly generated by the combustion of fossil fuels. Oxymethylene ethers (OMEs) are a series of liquid fuel additives that can be obtained from syngas, which is produced from the gasification of biomass. The blending of OMEs in conventional diesel fuel can reduce soot formation during combustion in a diesel engine. In this research, a process for the production of OMEs from woody biomass has been simulated. The process consists of several unit operations including biomass gasification, syngas cleanup,

---
[1] Corresponding author. Tel.: +1-780-492-7797.

  E-mail: Amit.Kumar@ualberta.ca (A. Kumar).

methanol production, and conversion of methanol to OMEs. The methodology involved the development of process models, the identification of the key process parameters affecting OME production based on the process model, and the development of an optimal process design for high OME yields. It was found that up to 9.02 tonnes day^{-1} of OME$_3$, OME$_4$, and OME$_5$ (which are suitable as diesel additives) can be produced from 277.3 tonnes day^{-1} of wet woody biomass. Furthermore, an optimal combination of the parameters, which was generated from the developed model, can greatly enhance OME production and thermodynamic efficiency. This model can further be used in a techno-economic assessment of the whole biomass conversion chain to produce OMEs. The results of this study can be helpful for petroleum-based fuel producers and policy makers in determining the most attractive pathways of converting bio-resources into liquid fuels.

Keywords: Biomass; gasification; methanol; oxymethylene ethers; diesel additive

1. Introduction

As a CO_2-neutral, renewable energy resource, biomass has the potential to reduce greenhouse gas (GHG) emissions, and it is expected that biomass-based energy will gradually substitute a portion of fossil fuel-based energy [1]. The potential end products that can be derived from biomass include liquid fuels, power, and heat [1-5]. Specifically, biomass-derived liquid fuels can be blended with petroleum-based diesel, thereby providing an environmentally friendly alternative to the GHG-intensive oil and gas industry.

Diesel engines are among the most common internal combustion (IC) engines, widely used in transportation, agriculture and other industrial applications. However, diesel exhaust contains toxic air contaminants such as nitrogen oxides and soot. Soot formation is particularly a problem

during diesel combustion. Adding biomass-based liquid fuels, mainly oxygenated compounds, to diesel fuels has been acknowledged as a solution to reduce soot formation [6]. That is because the chemical structure unit ($-O-CH_2-$) of the oxygenated compounds forms hydroperoxides in the initial stage of the combustion process. These hydroperoxides are further decomposed into hydroxide radicals. Subsequently, the soot precursors can be degraded by hydroxide radicals through oxidation [7]. Moreover, blending oxygenated compounds in diesel fuel can decrease NO_x emissions [8]. This is due to the lower combustion temperature when blending diesel with oxygenated compounds than that of solely conventional diesel combustion [8].

Oxygenated compounds that can be used as diesel substitutes or additives include dimethyl ether (DME), dimethoxymethane (DMM), and oxymethylene ethers (OMEs). One problem of using diesel/DME [9, 10] or diesel/DMM [11, 12] blends is that an engine modification is required. This is because DME or DMM may increase the fuel vapor pressure [9] and may also lower the fuel viscosity [9] and further reduce solubility at low temperatures [9, 10]. Because of the increased vapor pressure and limited miscibility with diesel, diesel/DME or diesel/DMM blends are not stable at normal pressure and an engine modification such as an additional pressurized tank or a modified fuel system is needed. OMEs with the chemical structure $CH_3-O-[CH_2-O-]_n-CH_3$ exhibit viscosities and boiling points closer to conventional diesel than either DME or DMM and are more suitable diesel additives; no changes are required to an engine when OMEs are used [13, 14]. In addition to not having to modify an engine when OMEs are blended with conventional diesel, OMEs have several other advantages that make it an attractive option as a fuel additive. Those advantages mainly include: faster ignition than diesel fuel, DME, and DMM due to higher cetane number; higher flash point than conventional diesel and hence are better to meet the security criterion [15]. Additionally, OMEs contain more oxygen than DME or DMM,

thus lower amounts of OMEs are required in a blend to reach a particular oxygen content [13]. However, OMEs have lower heating values than diesel fuel, and OMEs cost more to be produced than DME, DMM, and other oxygenates. But if the engine and system modification costs are considered, especially for DME, and further costs for storage, transportation, and safety of liquefied DME under pressure, the high production costs of OMEs can become acceptable.

Regarding the chain length, the most suitable OMEs to be blended into conventional diesel are those with $n=3,4,5$ (OME_3, OME_4 and OME_5) [6, 16-18]. A short chain length ($n=2$) cannot meet the security criterion due to a low flash point, and a long chain length ($n>5$) may clog the fuel system when mixed with conventional fuel due to solid precipitation [6, 16-18]. Thus, either experimental or modeling efforts should be done to find an optimal process for generating a high yield of OME_3, OME_4, and OME_5 from biomass feedstocks.

Methanol is a key building block during the whole process of producing OMEs from biomass, where biomass initially is converted into methanol, which can be further upgraded into OMEs. As producing methanol from biomass has been extensively investigated experimentally [19, 20] and through modeling [21-23], the further upgrading of methanol to OMEs becomes a more promising research area. Burger et al. [6] systematically reviewed the physical and chemical properties of OMEs as diesel additives followed by a conceptual proposal of the formation pathway of OMEs from DMM and trioxane (TRI). The proposed pathway was further investigated by the same research group in a stirred batch reactor, with detailed chemical equilibrium and reaction kinetics characterization [24]. An important intermediate during this process is formaldehyde (FA), which is produced from methanol through dehydrogenation. FA then reacts with methanol to form DMM, which is OME_n with $n=1$, through a heterogeneously catalyzed reactive distillation. Following this reaction, the other OMEs can be produced by

adding FA [24]. TRI is a stable cyclic trimer and a stable source of FA. The effect of different catalysts on the yields of different OMEs produced from methanol and TRI was also investigated [25] and showed that the acidic property of a catalyst influenced OME yield significantly, that is, a weak acidity catalyst leads to the formation of shorter chain length OMEs (OME_1, OME_2) and a strong acidity catalyst leads to the formation of longer chain length OMEs (OME_{3-8}).

Despite of the extensive studies on the methanol production from biomass, and some equilibrium, kinetic, and catalytic investigations on the methanol-to-OME process, studies on the whole process of OME production from biomass feedstock are still limited. The main purpose of this paper is to build a systematic model on the whole process of OME production from biomass, to test key parameters that affect the process, and to design an optimal process aimed at high OME (especially OME_3, OME_4, and OME_5) production from woody biomass. The developed model would further be used to conduct techno-economic and life-cycle assessment studies to determine the most economical and least GHG-intensive means of producing OMEs for blending them with petroleum-based fuel.

2. Modeling Description

2.1   Feedstock properties

The feedstock used in this study is a typical second-generation biomass, woodchips from whole forest trees. The detailed characteristics, including the proximate and ultimate analyses and the lower heating value (from the ECN Phyllis classification [26]), are shown in Table 1. The moisture content of woodchips was adjusted from 40% to 50% [1] due to the higher level of moisture in whole forest chips than that in forest residue and agricultural biomass. The feedstock biomass is considered as a non-conventional solid in the Aspen Plus simulation. The stream class

used in the process simulation is MIXCINC, which can handle all three stream types in the process: vapor-liquid, solid, and non-conventional stream.

Table 1

2.2 Modeling details

The process designed in this research for OME production from biomass via methanol building block is divided into four steps: (1) biomass gasification, which produces syngas; (2) raw syngas cleanup including steam reforming, waste gas removal, and H_2-CO ratio adjusting; (3) synthesis of methanol from clean syngas; and (4) conversion of methanol to OMEs over an acid catalyst.

All the models in this work for the various unit operations were developed in Aspen Plus [27]. The detailed modeling steps include whole process design, operating conditions input, and connections between different unit blocks. The schematic structure of the unit blocks included in the process model is shown in Fig. 1. There are three main steps in the investigation of the biomass-to-OME process: first, a base model that included all the unit operations was built and basic inputs for the process modeling were fixed. Second, key feedstock properties were identified and developed different steps in the biomass-to-OME process by building different modules in each step, and choosing a suitable property method for each module. Based on this model, the effects of key operating parameters for the process were investigated. Finally, a process design with the optimal combination of key operating parameters was proposed.

Fig. 1

2.2.1 Biomass gasification

The biomass gasification process is the first step for the whole designed biomass-to-OME plant. As shown in Fig. 1, generally the process can be described as the injection of air into dry biomass (woodchips in this case); raw syngas is produced and is delivered into the "Syngas cleanup and adjusting" section. Several thermo-chemical processes need to be considered in this section including drying, pyrolysis, combustion, and char gasification. Additional Fortran calculators were used to model those processes due to the complexity of the involved reactions. For the drying process, it is assumed that the moisture content is reduced from 50% to 28% [28, 29]. The energy used for the biomass drying is assumed to be provided by part of the energy released during biomass combustion. The inlet temperature for incoming biomass and air is assumed to be 25 °C, the atmospheric temperature. In our model, the Peng-Robinson (PENG-ROB) property method [30] was chosen for the dryer; this method is well suited for hydrocarbon processing applications. Dried biomass is first pyrolyzed into char, tar, and gases. The solid char from pyrolysis can be further gasified into gases using air or CO_2 as gasification agents. The CO_2 is mainly produced from biomass combustion.

A broad range of reactor types has been and continues to be used for gasification, including moving-bed gasifiers, fluidized-bed gasifiers and entrained-flow gasifiers [31]. In this study, a circulating fluidized-bed (CFB) gasifier was chosen; its advantages are high syngas production and wide fuel adaptability [32]. The feedstock mass flow for the gasifier is 3.21 kg s^{-1}, with a heat capacity of 26.37 MW (based on the LHV shown in Table 1), and the bed material is sand.

The drying and pyrolysis processes are simulated using stoichiometric reactors (RStoic), and the property method in the simulation is RK-SOAVE, which is recommended for hydrocarbon

processing applications [30]. A combination of an RYield reactor and an RGibbs reactor is adopted to model the char gasification process and combustion process, as shown in Fig. 1. The RYield and RGibbs block combination is selected because the Gibbs free energy of biomass cannot be calculated in Aspen Plus as it is a non-conventional solid, thus an RYield block is needed first to decompose the biomass into its constituent elements. Empirical equations are used to calculate gas, tar, and solid char yields [33] for the pyrolysis reaction in the RStoic. The pyrolysis gases include H_2O, CO_2, CO, H_2, some light hydrocarbons (CH_4, C_2H_4, C_2H_6), and other gases (NH_3, H_2S, HCl, SO_2, NO, N_2O, CHN-hydrogen cyanide). Tar compositions include C_6H_6, C_6H_6O, C_7H_8, $C_{10}H_8$ and longer chains with more than 10 carbon atoms. Hydrocarbons with a chain length longer than 10 are assumed to be removed after tar cracking and steam reforming. It is assumed that 32% N [34, 35], 46% S [35, 36], and 28% Cl [35, 37] remain in the solid char. Char reacts with both O_2 and CO_2 during char gasification.

2.2.2 Gas cleaning and H_2-CO ratio adjusting

The gas cleanup unit is mandatory as it removes tars, dust, and unwanted gases. In this research, conventional low temperature wet cleaning technology is modeled for syngas cleaning [38]. Tar is reduced through thermal cracking and steam reforming [39]. Thermal cracking of tar is considered to happen inside the gasifier since it requires a high temperature (about 1100 °C).

This reaction is characterized using the "tar cracking" block as shown in Fig. 1. Steam reforming is considered during the syngas cleaning process to further reduce tar. Finally, after thermal cracking and steam reforming, tar is broken down into lighter molecules like CO and H_2. In this research it is assumed that a bag filter is used to remove the dust contained in the raw syngas.

To achieve a high methanol and downstream OME yield, a high hydrogen content in syngas is required. Bio-syngas, on the contrary, is a CO_2-rich and H_2-deficient feed gas. There are several ways to adjust the ratio of the components H_2, CO, and CO_2 [40, 41]: a) water-gas shift reaction, b) methane reforming, c) carbon dioxide removing, and d) addition of hydrogen. Both the water-gas shift reaction and steam reforming are considered in this simulation to increase the H_2 yield. The water-gas shift reaction (Eq. 1) is simulated using a stoichiometric reactor (RStoic), using the PENG-ROB property method [30]. To determine the conversion rate of the water-gas shift reaction, the H_2-CO molar ratio is taken as 2:1 [30, 38], which is considered as the optimal ratio to maximize the methanol yield. Therefore the conversion rate is varied until the molar ratio is 2:1. To further increase the conversion rate of syngas into methanol, CO_2 is removed from the syngas with the intent that the $(H_2$-$CO_2)$-$(CO$+$CO_2)$ ratio comes closer to 2:1. However, some amount of CO_2 in the feed syngas is advantageous to increase methanol yield, mainly to maintain reaction equilibrium and catalyst activity [42]. It was found that a CO_2 volume fraction of 2% to 10% is suitable for methanol formation [43], and in this simulation, a specified level of CO_2 volume fraction at 5% was considered after the removal of CO_2 [38].

2.2.3 Production of methanol and formaldehyde

Two common methods used to produce methanol from biomass are biomass gasification into syngas with subsequent methanol synthesis and biomass anaerobic digestion. The former is attractive due to the higher carbon conversion rate [44]. A stoichiometric reactor (Rstoic) was chosen in this work to model methanol synthesis in a fixed-bed reactor. The yield of methanol synthesized from bio-syngas is highly dependent on the operation parameters [38]. A proper H_2-CO ratio adjusting section and a CO_2 removal section have been considered in the syngas cleaning and adjusting section for high methanol production. The reactor temperature is set at

300 °C for better catalyst activity, and the vapor-phase products from the methanol synthesis reactor are cooled to 32 °C to recover the methanol [42]. The conversion rate is set at 99% [38].

Formaldehyde (FA) is produced from methanol at a reactor temperature of 200 °C in the presence of air at a conversion rate of 60% [45]:

2.2.4 Synthesis of OMEs

The reaction chain involved in the production of OMEs from methanol and FA is illustrated in Fig. 2. Methanol, FA and water react to form a series of OME_n with different chain lengths and side products like glycols (Gly), hemi-formals/acetals (HF) and trioxane (Tri). However, OME_3, OME_4 and OME_5 are of major interest, since these are suitable for blending with conventional diesel. Blending OMEs with a short chain length in conventional diesel fails for safety reasons like low boiling and flash points and blending OMEs with long chain length can lead to clogging the fuel system [6, 16].

Fig. 2

Different feed compositions as shown in Table 2 were used at temperatures of 40, 60, 80, 100 and 120 °C, respectively, to identify the equilibrium parameters of the OME synthesis. A modified van't Hoff equation was used to fit the parameters *A* and *B* to the chemical equilibrium constants [46].

Table 2

The equilibrium parameters *A* and *B* are shown in Table 3 for reactions 4 and 8 (see Fig. 2) and are in good agreement with recently published data from Schmitz et al. [46].

Table 3

2.2.5 Experimental procedure for obtaining equilibrium parameters

The reactions were carried out in a stainless steel (1.4751) batch reactor with a maximum volume of 180 ml, a temperature resistance of 300 °C and a maximum pressure of 200 bar. Pressure and temperature were measured using an analog pressure gauge with an accuracy of 0.05 bar and a NiCr-Ni thermocouple with an accuracy of 1 °C. A valve at the bottom of the reactor was used for liquid phase sampling during the reaction. The valve was purged with the product before the sample was taken with a syringe. The sample was filtrated employing a polytetrafluoroethylene filter (0.2 μm pore width) and quenched with tetrahydrofuran (THF, AnalaR NORMAPUR®, 99.8%).

Reactants were methanol (Merck EMSURE®, purity = 99.9%) and p-formaldehyde (Merck, purity = 95%). Nitrobenzene (Sigma-Aldrich, purity = 99.0%) was used as internal standard for GC measurements, THF and 1-butanol (Merck EMSURE®, purity = 99.5%) were used as solvents. The ion exchanger Amberlyst 36 (Rohm and Haas, hydrogen form) was used as heterogeneous catalyst. The catalyst was dried under vacuum (3 mbar) for 24 h at 100 °C and stored under argon before use.

The equilibrium (methanol rate of change below 1×10^4 mol l^{-1} min^{-1}) was reached in all experiments within 5 h. For a homogenous phase, p-formaldehyde (p-FA) and methanol were mixed for two days under stirring at a temperature of 80 °C, before the catalyst was added to the reaction mixture and OME production took place.

A Hewlett Packard HP5890 gas chromatograph with an Agilent DB-5MS column (length = 30 m, diameter = 0.25 mm, film = 0.25 μm) and a HP 5971A mass selective detector was used for

the qualitative and quantitative analysis of the liquid samples. Synthesized and purified OMEs were utilized for calibration.

The concentration of the components FA, HF and Gly were calculated using the equilibrium parameters from Hahnenstein et al. [47]. The overall FA concentration was analyzed via sodium sulfite titration according to the method reported by Walker [45].

2.3   Model validation

Currently, few experimental works exist for the synthesis of OMEs using methanol as feedstock and no experimental work has been done on the production of OMEs from biomass, even on a laboratory scale. Therefore, we validated our model results in two separate parts, methanol production from biomass and OME production from methanol. Methanol production from biomass has been widely studied in the literature and therefore, the model result in this study is compared with that in the literature. The related yield of methanol from a unit of biomass can be calculated, on a wet basis, a dry basis, and a dry ash free (daf) basis. Table 4 gives the comparison of methanol yield with results from the literature considering the same conversion pathway (biomass gasification followed by methanol synthesis). The methanol yield in this model prediction were in perfect agreement with that in the literature [48] and the slight variation can be attributed to different biomass feedstocks (rice straw, wood chips, and crop residues) and operating conditions.

Table 4

The second part of our model (OME production from methanol and formaldehyde) was validated using the experimental results in terms of equilibrium constants (Table 3). For the simulation, p-

FA was defined as 95 % FA containing 5 % of water. The mole fraction-based chemical equilibrium constants of reactions 1, 2, 5 and 7 (Fig. 2) were taken from Hahnenstein et al. [47].

In the model, FA was produced from methanol at a conversion rate of 60% to maintain the same ratio as that of the experiment. The resulting OME mass fractions from experiment were compared with those of the model and the corresponding errors were calculated. Table 5 shows the mass fractions of OMEs 1 to 5 for the experimental and the modelling results with a maximum error of 3%. Only small amounts of higher OME (n>5) exists. Therefore, the model predictions were found to be in good agreement with the experimental results.

Table 5

3. Results and Discussion

3.1 Key operating parameters

Different operating conditions will lead to differences in OMEs production. In this study, various operating parameters aimed at high OMEs yield were tested and evaluated. The key operating parameters considered in this study are equivalence ratio, H_2-CO ratio, and extra water injection.

3.1.1 Equivalence ratio

Air was chosen as oxidant for the gasification process and a key parameter that represents the amount of air supply is the air-fuel equivalence ratio (λ). The air-fuel equivalence ratio is defined as the actual air-fuel mass ratio divided by the air-fuel mass ratio at stoichiometric oxidation [49].

Since the energy needed for pyrolysis and gasification is provided by biomass combustion, actual air flow has a strong influence on the biomass-gasified fraction and the gasification temperature. Fig. 3 shows the influence of the equivalence ratio on OMEs production. It shows the temperature change when the Lambda increases from 0.07 to 1.05. The gasification temperature increases at the stage of uncompleted combustion (λ<1). This is because more biomass is combusted and more energy is released [50]. The gasification temperature starts decreasing when the combustion is complete (λ≥1), mainly due to increasing amounts of air injection. In the uncompleted combustion stage, the gasification temperature increases significantly when the Lambda is less than 0.45. This temperature starts to level off when a Lambda is larger than 0.45. The main reason for the slower rate of temperature increase is that part of the energy released is used to provide energy to heat N_2 in the air and the bed materials in the CFB [50]. The total OMEs 1-8 in Fig. 3 refer to the summation of OME1, OME2…, and OME 8 produced. The total OMEs 3-5 show the amount of OME that can be readily blended with diesel without any modification to the engine.

Fig. 3

OMEs yields are influenced by the gasification temperature. The production of OME first increased with increasing gasification temperature and start decreasing after reaching a maximum point at 998 K. The present model shows that when the actual air flow is about 27% of stoichiometric air, OMEs production is at its maximum. For a fixed feedstock flow rate (3.21 kg s^{-1}), the stoichiometric air flow is 12.25 kg s^{-1}, and the optimal air flow is 3.31 kg s^{-1}.

3.1.2 H_2-CO molar ratio adjusting

A suitable H_2-CO ratio is needed for higher methanol yield. In this work, the H_2-CO ratio is adjusted by changing the water-gas shift reaction conversion rate, which was defined as the mass flow of reacted CO during the water-gas shift reaction divided by the mass flow of total CO in the raw syngas. OME production and H_2-CO ratio change with variations in the conversion rate of the water-gas shift reaction is shown in Fig. 4. Maximum methanol is produced at a H_2-CO ratio of around 2:1, therefore the highest OME_{1-8}, OME_{2-8}, and OME_{3-5} yield can be obtained at the same ratio as shown in Figure 4 [30, 38]. To reach those criteria, the required water-gas shift reaction conversion rate is around 0.227 (see Fig. 4) and was concluded as the optimal water-gas shift reaction conversion rate for the current case. The reason for the existence of an optimal water-gas shift reaction conversion rate is that the H_2-CO ratio is normally lower than 2:1, which can be adjusted by adding water during the process to convert part of CO into H_2, however, if the conversion rate is high, that is, a higher H_2-CO ratio than 2:1, the methanol yield will be reduced due to a lack of CO and thus the downstream OME yield will be reduced. This optimal conversion rate should be varied with different conditions, for example, for feedstock with a high moisture content, the existence of vapors in the system already convert part of the CO into H_2, thus in this case, a low water-gas shift reaction conversion rate is needed.

Fig. 4

3.1.3 Water injection

Some extra makeup water may be needed to produce OMEs from biomass. The injected water is used for steam reforming and the water-gas shift reaction. However, excessive water (water remaining after steam reforming and the water-gas shift reaction) in the system will form some side products, which will make OME purification difficult [13, 25]. At the same time, water

inhibits the production of formaldehyde from methanol, thereby reducing OME yield [30]. Important factors that influence the amount of water injection are feedstock moisture content and biomass pre-drying [30]. For the present case, no extra water is needed since the moisture content in the feedstock is high (50 %).

3.2 An optimal process design

Based on the analysis of the key operating parameters in section 3.1, the following optimal process aiming at high OMEs yield is proposed for a biomass-to-OME process with 3.21 kg s^{-1} biomass feedstock input: 3.31 kg s^{-1} air and a H$_2$-CO molar ratio of 2:1 with a water-gas shift reaction conversion of 0.227 with no makeup water injection. With this combination of parameters, optimal syngas quality, maximum methanol yield, and maximum OME yield can be obtained.

Raw syngas is the gaseous product from the gasifier, and adjusted syngas is the syngas after H$_2$-CO adjusting following the water-gas shift reaction and tar reforming. The molar fraction of different gas components in both raw syngas and adjusted syngas is shown in Fig. 5. Raw syngas has a high water content, due to the feedstock's high moisture content. After adjusting, a large amount of water is removed through the water-gas shift reaction. Both raw syngas and adjusted syngas are high in nitrogen, mainly from air. High nitrogen content is a problem that can be avoided by using pure oxygen as a gasification agent; however, the cost of oxygen purification needs to be considered in that case. The molar fractions of both CO and H$_2$ got increased after adjusting, mainly from tar cracking and steam reforming reaction. The H$_2$-CO molar ratio in raw syngas is 1.2:1 and increases to 2:1 after adjusting, with a water gas shift reaction conversion rate of 0.227, as mentioned above. Small amounts of hydrocarbons (C$_n$H$_m$) and other gases are generated, mainly through the tar reforming reaction.

Fig. 5

The mass flow of the optimal process is shown in full in Fig. 6. For a woodchip plant with a capacity of 277.3 tonnes day^{-1} (which was 3.21 kg s^{-1} in the model), the optimal air mass flow rate is 285.95 tonnes day^{-1} under the condition that all the energy required for biomass drying, pyrolysis, and gasification is from the biomass combustion itself. The H_2-CO molar ratio in the raw syngas is 1.2:1, and after syngas cleaning and adjusting, the ratio is 2:1, which is suitable for methanol production. The water-gas shift reaction conversion rate required for adjusting is 0.227. Methanol yield is 79.08 tonnes day^{-1}, and air input for the formaldehyde synthesis prior is 172.8 tonnes day^{-1} (79% N_2 and 21% O_2 mole fraction). The total OME$_{1-8}$ yield is 30.20 tonnes day^{-1} with OME$_3$, OME$_4$, and OME$_5$ yields of 4.75, 2.74 and 1.53 tonnes day^{-1} respectively.

Fig. 6

4. Conclusions

In this study, a process model for the production of oxymethylene ethers (OMEs) from woody biomass was developed and simulated. The simulation involved the gasification of woody biomass to produce syngas, followed by methanol and then OME. The methanol to OME pathway was validated with experimental results and the model predictions were found to be in good agreement with the experimental results with a maximum error of 3%. An optimal design of OME production from woody biomass was developed in this research, and it was found that several key operating parameters significantly affect OMEs yield. The optimal value for actual air requirement is 27% of the stoichiometric value. The water-gas shift reaction conversion should reach 22.7% to ensure that the H_2-CO molar ratio is 2:1 for maximum methanol production. No makeup water is needed for either steam reforming or the water-gas shift reaction

due to the high moisture content of the feedstock. With a woodchip plant capacity of 277.3 tonnes day^{-1}, 30.20 tonnes day^{-1} of OME$_{1-8}$ can be obtained, with 9.02 tonnes day^{-1} of OME$_{3-5}$. The results of this study will be helpful for petroleum-based fuel producers and policy makers on how much OME can be produced from biomass-based feedstocks for blending with diesel fuels.

Acknowledgments

References

[1] Kumar A, Cameron JB, Flynn PC. Biomass power cost and optimum plant size in western Canada. Biomass Bioenerg. 2003; 24(6): 445-64.

[2] Sarkar S, Kumar A. Techno-economic assessment of biohydrogen production from forest biomass in Western Canada. Transactions of the ASABE. 2009; 52(2): 519-30.

[3] Sarkar S, Kumar A. Biohydrogen production from forest and agricultural residues for upgrading of bitumen from oil sands. Energy. 2010; 35(2): 582-91.

[4] Sarkar S, Kumar A, Sultana A. Biofuels and biochemicals production from forest biomass in Western Canada. Energy. 2011; 36(10): 6251-62.

[5] Shahrukh H, Oyedun AO, Kumar A, Ghiasi B, Kumar L, Sokhansanj S. Net energy ratio for the production of steam pretreated biomass-based pellets. Biomass Bioenerg. 2015; 80(0): 286-97.

[6] Burger J, Siegert M, Ströfer E, Hasse H. Poly (oxymethylene) dimethyl ethers as components of tailored diesel fuel: Properties, synthesis and purification concepts. Fuel. 2010; 89(11): 3315-9.

[7] Lahaye J, Prado G. Soot in combustion systems and its toxic properties. New York : Published in cooperation with NATO Scientific Affairs Division Plenum Press; 1983.

[8] Buchholz BA, Cheng ASE, Dibble RW. Isotopic Tracing of Bio-Derived Carbon from Ethanol-in-Diesel Blends in the Emissions of a Diesel Engine. SAE Technical Paper No. 2002-01-1704; 2002.

[9] Ying W, Genbao L, Wei Z, Longbao Z. Study on the application of DME/diesel blends in a diesel engine. Fuel Process Technol 2008; 89(12): 1272-80.

[10] Zhao X, Ren M, Liu Z. Critical solubility of dimethyl ether (DME)+diesel fuel and dimethyl carbonate (DMC)+diesel fuel. Fuel. 2005; 84(18): 2380-3.

[11] Ren Y, Huang ZH, Jiang DM, Liu LX, Zeng K, Liu B, Wang XB. Engine performance and emission characteristics of a compression ignition engine fuelled with diesel/dimethoxymethane blends. P I MECH ENG D-J AUT. 2005; 219(7): 905-14.

[12] Vertin KD, Ohi JM, Naegeli DW, Childress KH, Hagen GP, McCarthy CI, Cheng AS, Dibble RW. Methylal and Methylal-Diesel Blended Fuels from Use In Compression-Ignition Engines. SAE Technical Paper No. 1999-01-1508; 1999.

[13] Burger J, Siegert M, Ströfer E, Hasse H. Poly(oxymethylene) dimethyl ethers as components of tailored diesel fuel: Properties, synthesis and purification concepts. Fuel. 2010; 89(11): 3315-9.

[14] Burger J, Ströfer E, Hasse H. Production process for diesel fuel components poly(oxymethylene) dimethyl ethers from methane-based products by hierarchical optimization with varying model depth. Chem Eng Res Des 2013; 91(12): 2648-62.

[15] Natarajan M, Frame EA, Naegeli DW, Asmus T, Clark W, Garbak J, Manuel A, González D, Liney E, Piel W, Wallace JP. Oxygenates for Advanced Petroleum-Based Diesel Fuels: Part 1. Screening and Selection Methodology for the Oxygenates. SAE Technical Paper No. 2001-01-3631; 2001.

[16] Lumpp B, Rothe D, Pastötter C, Lämmermann R, Jacob E. Oxymethylene ethers as diesel fuel additives of the future. MTZ worldwide eMagazine. 2011;72(3):34-8.

[17] Pellegrini L, Marchionna M, Patrini R, Beatrice C, Giacomo ND, Guido C. Combustion Behaviour and Emission Performance of Neat and Blended Polyoxymethylene Dimethyl Ethers in a Light-Duty Diesel Engine SAE Technical Paper No. 2012-01-1053; 2012.

[18] Pellegrini L, Marchionna M, Patrini R, Salvatore F. Emission Performance of Neat and Blended Polyoxymethylene Dimethyl Ethers in an Old Light-Duty Diesel Car SAE Technical Paper No. 2013-01-1035; 2013.

[19] Yin X, Leung DYC, Chang J, Wang J, Fu Y, Wu C. Characteristics of the Synthesis of Methanol Using Biomass-Derived Syngas. Energy Fuel 2005; 19(1): 305-10.

[20] Brachi P, Chirone R, Miccio F, Miccio M, Picarelli A, Ruoppolo G. Fluidized bed co-gasification of biomass and polymeric wastes for a flexible end-use of the syngas: Focus on bio-methanol. Fuel. 2014; 128(0): 88-98.

[21] Phillips SD, Tarud JK, Biddy MJ, Dutta A. Gasoline from Woody Biomass via Thermochemical Gasification, Methanol Synthesis, and Methanol-to-Gasoline Technologies: A Technoeconomic Analysis. Ind Eng Chem Res 2011; 50(20): 11734-45.

[22] Feng W, Ji P, Chen B, Zheng D. Analysis of Methanol Production from Biomass Gasification. Chem Eng Technol 2011; 34(2): 307-17.

[23] Hamelinck CN, Faaij APC. Future prospects for production of methanol and hydrogen from biomass. J Power Sources. 2002; 111(1): 1-22.

[24] Burger J, Ströfer E, Hasse H. Chemical Equilibrium and Reaction Kinetics of the Heterogeneously Catalyzed Formation of Poly(oxymethylene) Dimethyl Ethers from Methylal and Trioxane. Ind Eng Chem Res 2012; 51(39): 12751-61.

[25] Zhao Q, Wang H, Qin Z-f, Wu Z-w, Wu J-b, Fan W-b, et al. Synthesis of polyoxymethylene dimethyl ethers from methanol and trioxymethylene with molecular sieves as catalysts. J Fuel Chem Technol 2011; 39(12): 918-23.

[26] ECN [Internet]. Phyllis database [Cited January 15 2015]. Available from: http://www.ecn.nl/phyllis/

[27] Aspen P. User Guide. Version 84. Burlington, MA: Aspen Technology Inc.; 2014.

[28] Gebreegziabher T, Oyedun AO, Hui CW. Optimum biomass drying for combustion–A modeling approach. Energy. 2013; 53(1): 67-73.

[29] Luk HT, Lam TYG, Oyedun AO, Gebreegziabher T, Hui CW. Drying of biomass for power generation: A case study on power generation from empty fruit bunch. Energy. 2013; 63: 205-15.

[30] Johansson E. Process integration study of biomass-tomethanol (via gasification) and methanol-toolefins (MTO) processes in an existing steam cracker plant. [dissertation]. Göteborg (Sweden): Chalmers University of Technology; 2013.

[31] Basu P. Chapter 8 - Design of Biomass Gasifiers. In: Basu P, editor. Biomass Gasification, Pyrolysis and Torrefaction. 2nd ed. Boston: Academic Press; 2013. p. 249-313.

[32] Li X, Grace J, Lim C, Watkinson A, Chen H, Kim J. Biomass gasification in a circulating fluidized bed. Biomass Bioenerg 2004; 26(2): 171-93.

[33] Neves D, Thunman H, Matos A, Tarelho L, Gómez-Barea A. Characterization and prediction of biomass pyrolysis products. Prog Energ Combust 2011; 37(5): 611-30.

[34] Winter F, Wartha C, Löffler G, Hofbauer H. The NO and N_2O formation mechanism during devolatilization and char combustion under fluidized-bed conditions. Symp Int Combust Proc 1996; 26(2): 3325-34.

[35] Francois J, Abdelouahed L, Mauviel G, Patisson F, Mirgaux O, Rogaume C, et al. Detailed process modeling of a wood gasification combined heat and power plant. Biomass Bioenerg 2013; 51(0): 68-82.

[36] Knudsen JN, Jensen PA, Lin W, Frandsen FJ, Dam-Johansen K. Sulfur Transformations during Thermal Conversion of Herbaceous Biomass. Energy Fuel 2004; 18(3): 810-9.

[37] Jensen PA, Frandsen FJ, Dam-Johansen K, Sander B. Experimental Investigation of the Transformation and Release to Gas Phase of Potassium and Chlorine during Straw Pyrolysis. Energy Fuel 2000; 14(6): 1280-5.

[38] Phillips SD. Gasoline from wood via integrated gasification, synthesis, and methanol-to-gasoline technologies. Colorado: National Renewable Energy Laboratory (NREL). 2011. 115p. Report No. NREL/TP-5100-47594.

[39] Delgado J, Aznar MP, Corella J. Calcined Dolomite, Magnesite, and Calcite for Cleaning Hot Gas from a Fluidized Bed Biomass Gasifier with Steam: Life and Usefulness. Ind Eng Chem Res 1996; 35(10): 3637-43.

[40] Gallucci F, Basile A, Drioli E. Methanol as an Energy Source and/or Energy Carrier in Membrane Processes. Sep Purif Rev 2007; 36(2): 175-202.

[41] Puerari F, Bosio B, Heyen G. Energy efficiency optimisation in different plant solutions for methanol production from biomass gasification. Chem Eng Trans 2014; 301-6.

[42] Lee S. Methanol synthesis technology. Florida: CRC Press Inc.; 1989.

[43] Air Products Liquid Phase Conversion Company. Economic analysis LPMEOH process as an add-on to integrated gasification combined cycle (IGCC) for co-production. Report prepared by Air Products & Chemicals Inc. for the U.S. Department of Energy. Pennsylvania: Report No. DE-FC22-92PC90543; 1998.

[44] Vertes AA, Qureshi N, Yukawa H, Blaschek HP, editors. Biomass to biofuels: strategies for global industries. Chichester, U.K. : Wiley; 2010.

[45] Walker JF. Formaldehyde. New York: Reinhold publishing corporation; 1944.

[46] Schmitz N, Homberg F, Berje Jr, Burger J, Hasse H. Chemical Equilibrium of the Synthesis of Poly (oxymethylene) Dimethyl Ethers from Formaldehyde and Methanol in Aqueous Solutions. Ind Eng Chem Res. 2015; 54(25): 6409-17.

[47] Hahnenstein I, Albert M, Hasse H, Kreiter CG, Maurer G. NMR spectroscopic and densimetric study of reaction kinetics of formaldehyde polymer formation in water, deuterium oxide, and methanol. Ind Eng Chem Res. 1995; 34(2): 440-50.

[48] Nakagawa H, Sakai M, Harada T, Ichinose T, Takeno K, Yakushido K, Kobayashi M, Matsumoto S. Biomethanol production from forage grasses, trees, and crop residues. In Bernardes MADS, editor. Biofuel's Engineering Process Technology. Intech; 2011 Available from: http://www.intechopen.com/books/biofuel-s-engineering-process-technology/biomethanol-production-from-forage-grasses-trees-and-crop-residues.

[49] Stec AA, Hull TR, Lebek K, Purser J, Purser D. The effect of temperature and ventilation condition on the toxic product yields from burning polymers. Fire Materials. 2008; 32(1): 49-60.

[50] Lackner M. Combustion: In: Ullmann's Encyclopedia of Industrial Chemistry. Wiley Online Library; 2013. Available from:

http://onlinelibrary.wiley.com/doi/10.1002/14356007.b03_14.pub3/full.

Table 1: Characteristics of woodchip feedstock [26]

Proximate Analysis (wt %) (dry basis)							*LHV (dry basis)*
Moisture		Fixed Carbon		Volatile Matter		Ash	
50.0		39.3		59.8		0.9	
Ultimate Analysis (wt %) (dry basis)							16.43 MJ kg^{-1}
Ash	C	H	N	Cl	S	O	
0.9	48.6	6	0.14	0.005	0.02	44.335	

Table 2: Compositions of the educt mixtures for the calculation of the equilibrium parameters.

Experiment	Methanol (wt. %)	Formaldehyde (wt. %)	Water (wt. %)
1	66.5	31.4	2.1
2	49.9	47.0	3.2
3	40.7	55.6	3.7
4	38.6	52.7	8.8
5	37.0	50.5	12.5
6	32.5	44.3	23.2
7	36.7	50.1	13.2

Table 3: Equilibrium parameters based on mole fractions.

Reaction	A	B
(4, n = 1)	-0.7576	875.6
(4, n = 2)	-0.9705	908.3
(4, n = 3)	-1.1832	941.0
(4, n = 4)	-1.3961	973.8
(4, n = 5)	-1.6088	1006.4
(4, n = 6)	-1.8217	1039.1
(4, n = 7)	-2.0345	1071.8
(4, n = 8)	-2.2472	1104.5
(4, n = 9)	-2.4600	1137.2
(4, n = 10)	-2.6728	1169.9
(8, n > 0)	-2.4624	3041.5

Table 4: Comparison of methanol yield with results from the literature

	kg kg^{-1} (wet) biomass	kg kg^{-1} (dry) biomass	kg kg^{-1} (daf) biomass
This model	0.285	0.570	0.575
Nakagawa [48]	0.36-0.55	0.35-0.60	0.45-0.60
Vertes [44]	---	0.49	---
Johansson [30]	---	0.515	---

Table 5: Comparison of experimental OME mass fractions with calculated mass fractions from the model.

OMEs	Experimental, $x_{exp.}$ (wt. %)	Aspen model, $x_{model.}$ (wt. %)	Error (%)
OME 1	16.36	15.95	2.51
OME 2	9.90	10.02	1.16
OME 3	5.89	5.98	1.68
OME 4	3.27	3.30	0.81
OME 5	1.64	1.69	3.02

Figures
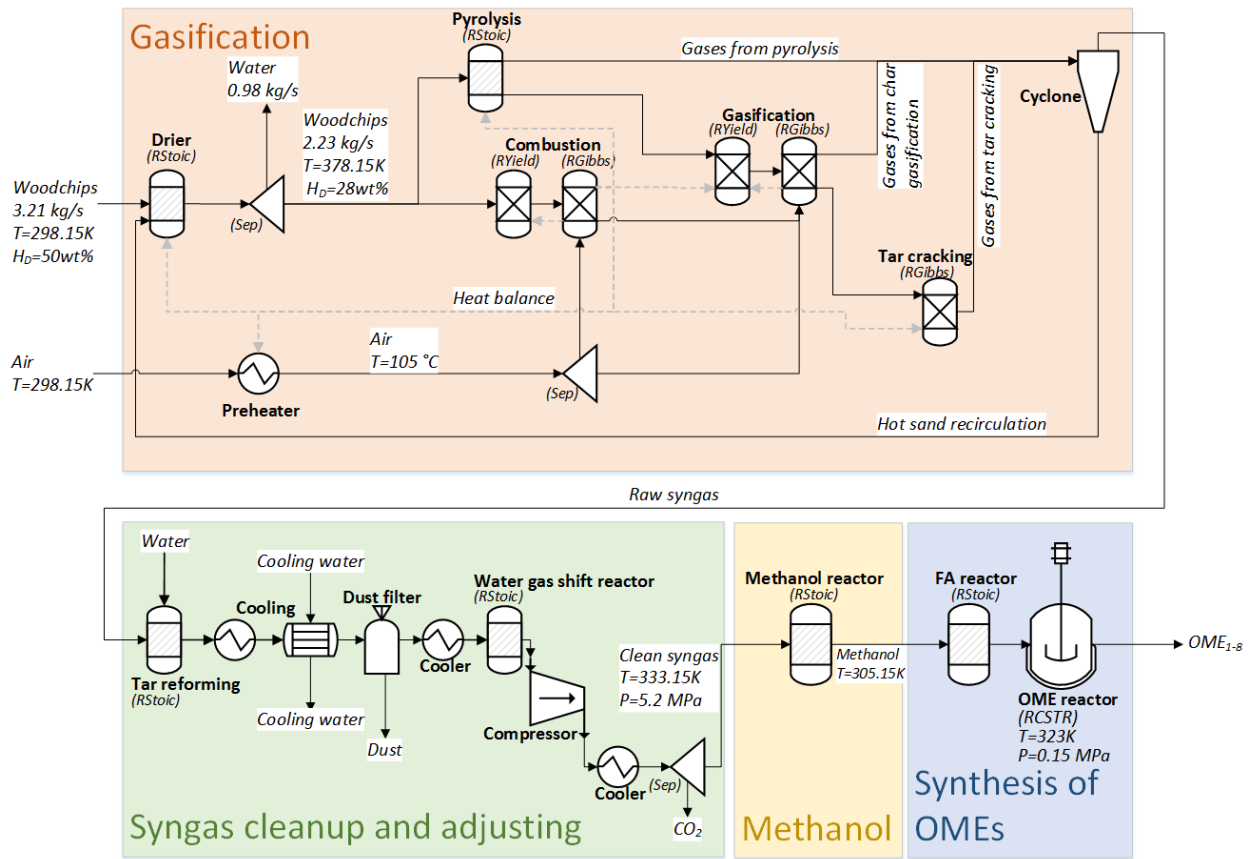
Fig. 1: Detailed Aspen Plus flow sheet for the biomass-to-OME process.

$$H_2O \quad + \quad H_2C{=}O \;\rightleftharpoons\; HO{-}CH_2{-}OH \tag{1}$$

FA   Gly

$$H_3C{-}OH \quad + \quad H_2C{=}O \;\rightleftharpoons\; CH_3{-}O{-}CH_2{-}OH \tag{2}$$

MeOH   FA   HF

$$3\; H_2C{=}O \;\rightleftharpoons\; \text{(trioxane ring)} \tag{3}$$

FA   Tri

$$HO{-}(CH_2O)_n{-}H \;+\; H_3C{-}OH \rightleftharpoons CH_3{-}O{-}(CH_2O)_n{-}CH_3 \;+\; H_2O \tag{4}$$

HF   MeOH   OME

$$HO{-}(CH_2O)_n{-}H \;+\; H_2C{=}O \rightleftharpoons HO{-}(CH_2O)_{n+1}{-}H \tag{5}$$

HF   FA   HF

$$HO{-}(CH_2O)_n{-}H \;+\; H_3C{-}OH \rightleftharpoons HO{-}(CH_2O)_n{-}CH_3 \;+\; H_2O \tag{6}$$

Gly   MeOH   HF

$$HO{-}(CH_2O)_n{-}H \;+\; H_2C{=}O \rightleftharpoons HO{-}(CH_2O)_{n+1}{-}H \tag{7}$$

Gly   FA   Gly

$$CH_3{-}O{-}(CH_2O)_n{-}CH_3 \;+\; H_2C{=}O \rightleftharpoons CH_3{-}O{-}(CH_2O)_{n+1}{-}CH_3 \tag{8}$$

OME   FA   OME
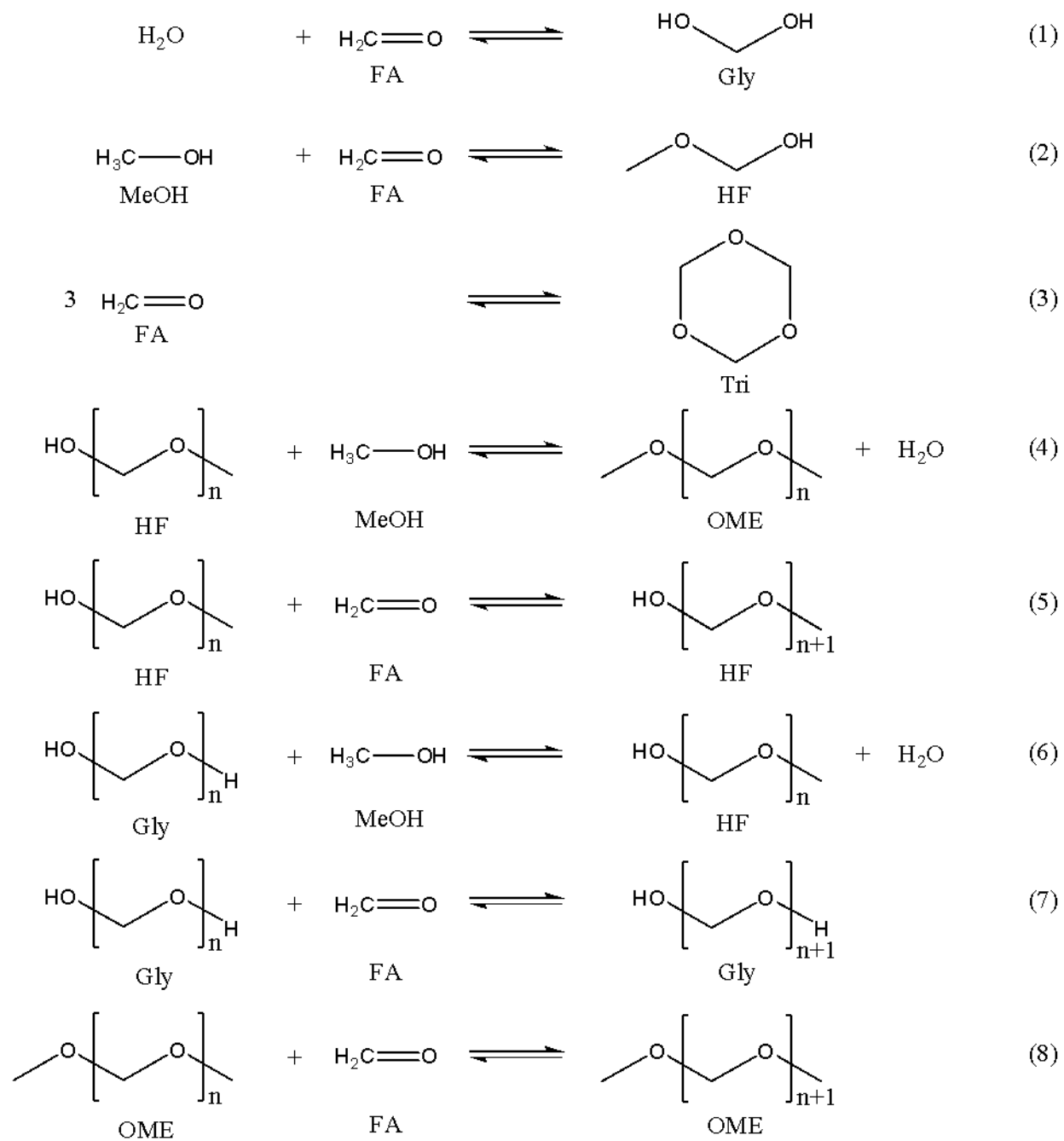
Fig. 2: Reactions for the production of OMEs from methanol and formaldehyde (FA: formaldehyde, Gly: glycols, Tri: trioxane, HF: hemi-formals/hemiacetals, OME: oxymethylene ethers, MeOH: methanol)
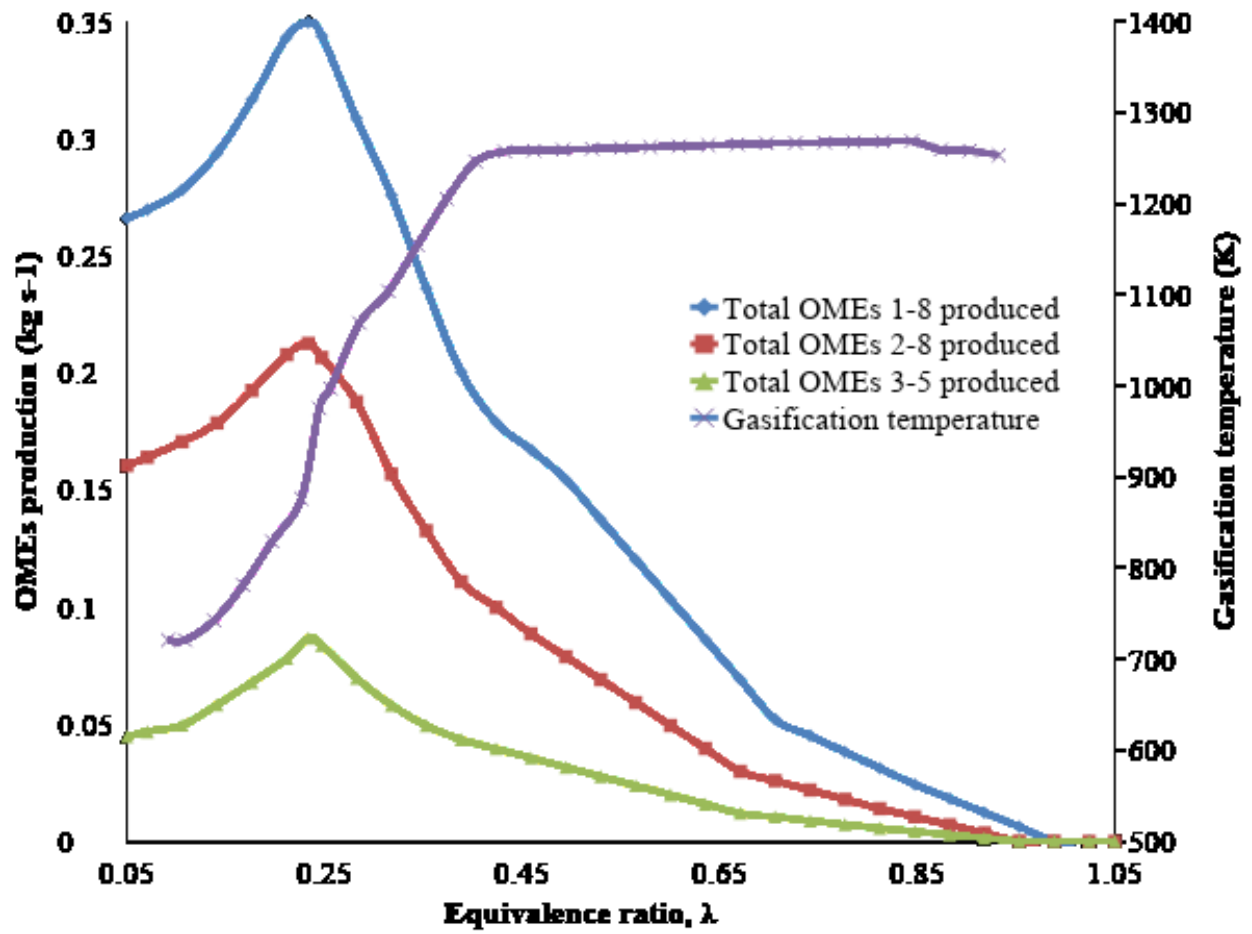
Fig. 3: The influence of the equivalence ratio on gasification temperature, OMEs yield
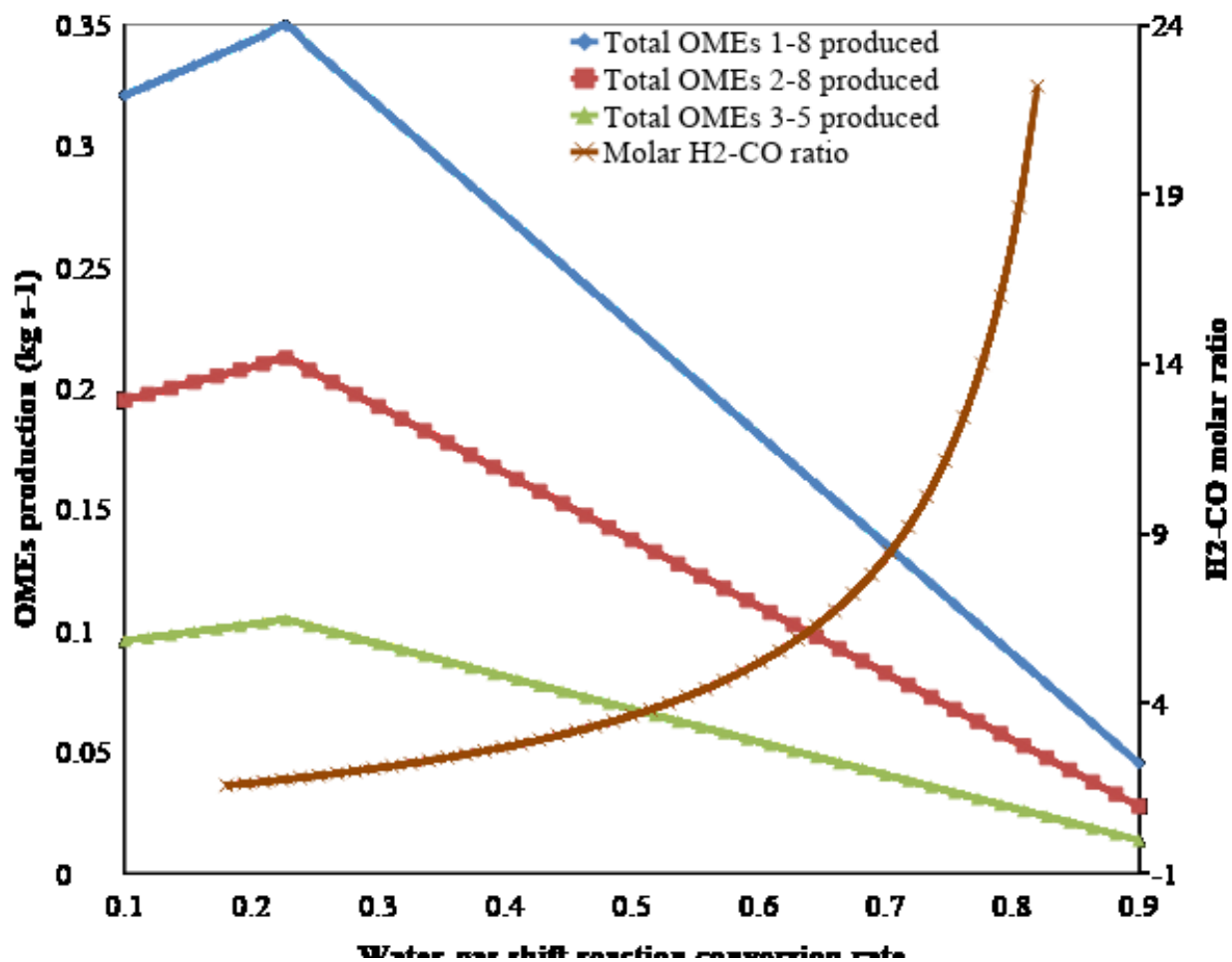
Fig. 4: The influence of the water-gas shift reaction conversion rate on the H$_2$-CO molar ratio and OMEs yield.
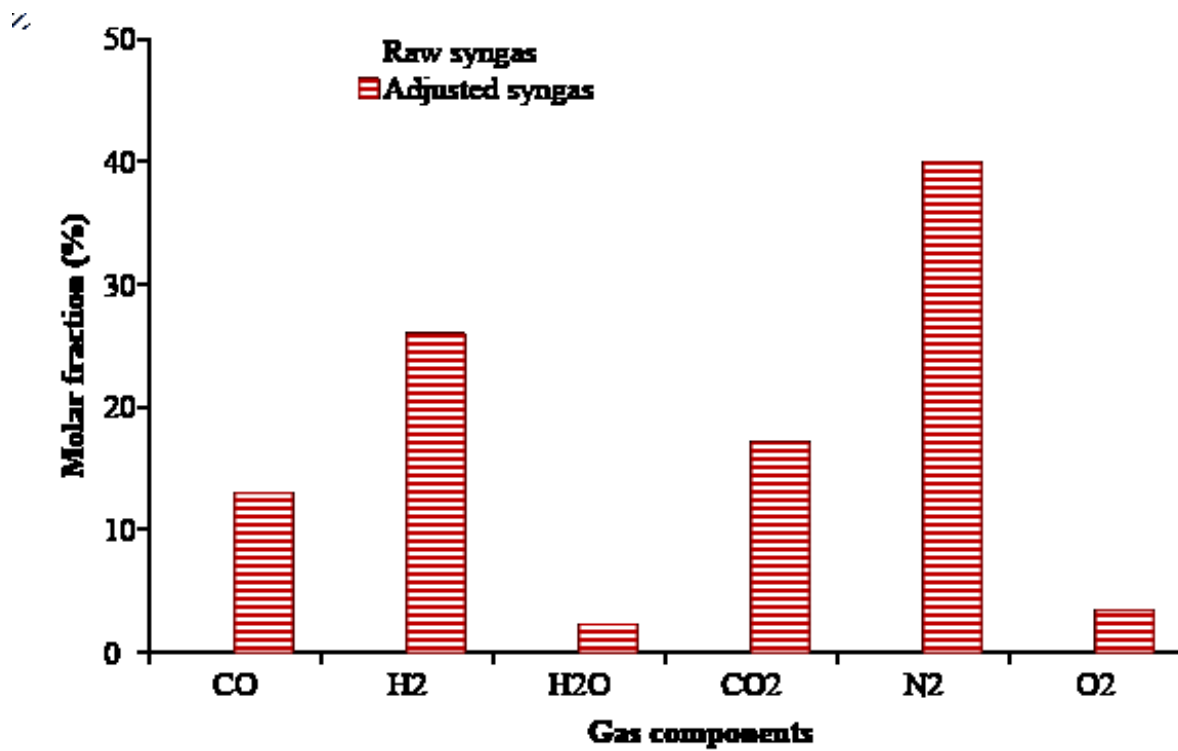
Fig. 5: The molar fraction of different gas components in both raw syngas and adjusted syngas.
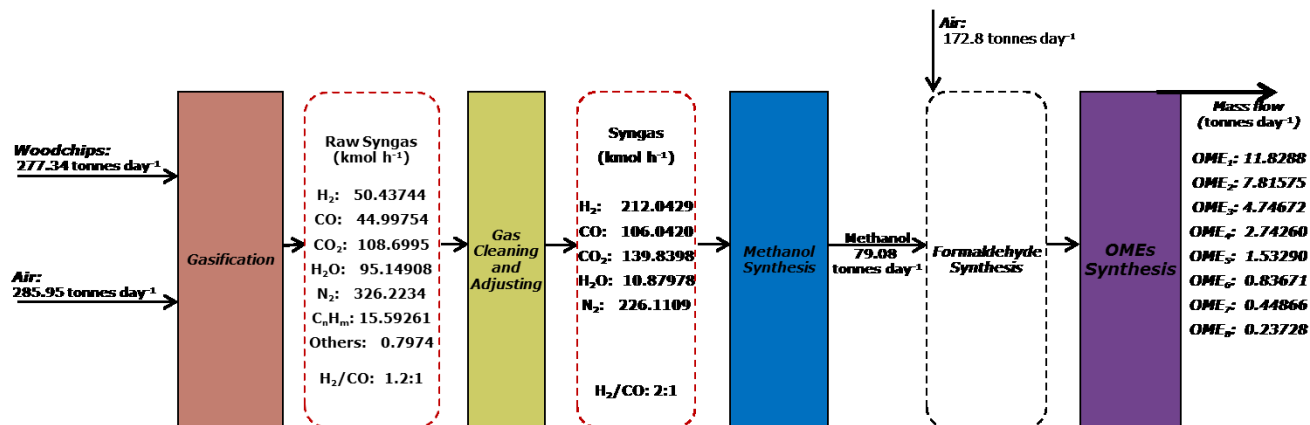
Fig. 6: The mass flow of the designed optimal process for OMEs production from woody biomass